Accepted Manuscript

A multifunctional material based on co-electrospinning for developing biosensors with optical oxygen transduction

Teresa Ramon-Marquez, Antonio L. Medina-Castillo, Naveen Nagiah, Alberto Fernandez-Gutierrez, Jorge F. Fernandez-Sanchez

PII: S0003-2670(18)30199-5

DOI: 10.1016/j.aca.2018.02.010

Reference: ACA 235726

To appear in: *Analytica Chimica Acta*

Received Date: 28 July 2017

Revised Date: 14 December 2017

Accepted Date: 6 February 2018

Please cite this article as: T. Ramon-Marquez, A.L. Medina-Castillo, N. Nagiah, A. Fernandez-Gutierrez, J.F. Fernandez-Sanchez, A multifunctional material based on co-electrospinning for developing biosensors with optical oxygen transduction, *Analytica Chimica Acta* (2018), doi: 10.1016/j.aca.2018.02.010.

A multifunctional material based on co-electrospinning for developing biosensors with optical oxygen transduction

Teresa Ramon-Marquez[a], *Antonio L. Medina-Castillo*[b,*], *Naveen Nagiah*[b], *Alberto Fernandez-Gutierrez*[a], *Jorge F. Fernandez-Sanchez*[a,**]

[1] Department of Analytical Chemistry, University of Granada, Avd. Fuentenueva s/n, 18071 Granada, Spain.

[2] NanoMyP®, Nanomateriales y Polimeros S.L., Spin-Off company of the UGR, BIC building, Avd. Innovacion 1, E-18016, Granada, Spain.

* Corresponding author. Nanomateriales y Polímeros S.L.

** Corresponding author. University of Granada Tel: +34958637114

E-mail addresses: amedina@nanomyp.com (A.L. Medina-Castillo), jffernan@ugr.es (J.F. Fernandez-Sanchez).

ABSTRACT

A multifunctional material based on co-electrospinning has been developed as a basic material for the development of biosensors with optical oxygen transduction. It is based on coaxial nanofibres: inner fibres containing an oxygen sensitive dye and outer fibres containing aldehyde groups to allow the formation of Schiff bases with the amino groups of the enzyme. The resulting material preserves the oxygen sensing properties of the inner optical transducer as well as exhibits a high capacity for immobilizing molecules on its surface.

Uricase has been selected as model enzyme and several parameters (temperature, pH, reaction time, buffer, and enzyme concentration) have been optimised to demonstrate the versatility of this novel multifunctional material in the development of biosensors with optical oxygen transduction for determining uric acid in serum samples. It suggests that the proposed multifunctional material can provide a promising multifunctional platform for biosensing applications.

Keywords: Multifunctional material; Nanotechnology; Oxygen transduction; Optical biosensor; Uric acid.

1. Introduction

The development of advanced multifunctional platforms with sensing properties based on new nanomaterials has attracted great interest in the past few years due to their tuneable physical, chemical, optical, mechanical and electronic properties, versatility, applicability in many different fields and, in some cases, biocompatibility and biodegradability [1, 2].

Advances in nanotechnology in recent years have stimulated the fast development of new nanomaterials with multiple functions and shapes (nanotubes [3], nanofibres [4], nanoparticles [5], nanocages [6], etc.), and made with a variety of materials (carbon [7], silicon [8], metals [9], polymers [10, 11]). Furthermore, the high capacity of modification of these nanomaterials allows functionalising their surface with multiple chemical groups that improve their ability to attach (bio)molecules. This modification results in huge number of applications in catalysis, biosensing, bioimaging, drug delivery and biomedicine [12, 13].

Among the wide diversity of novel functional nanomaterials, nanofibres membranes prepared by electrospinning technique offer several advantages such as high surface-to-volume ratio, controllable morphology, pore size, porosity and flexibility, and they can be fabricated as long or short fibres with modifiable orientation to provide a wide variety of sizes and shapes, which can lead to the fabrication of smart membranes [14, 15]. Because of these improved properties, nanofibres membranes could be very promising materials for developing biosensors [16, 17]. In addition, co-electrospinning technique allows one-step fabrication of multifunctional coaxial micro- and nano-fibre membranes which generate two different chemical environments that increase the functionality of these nanofibres [18, 19] as well as their applicability [20, 21], including sensing applications [20].

On the other hand, the use of optical oxygen transduction has been widely applied on the development of biosensors because it is simple, rapid and high sensitive and there is available a huge number of systems to do it [22, 23]. The monitoring of an enzymatic reaction by using oxygen transduction requires an increase or a decrease in the oxygen concentration, which has to be produced during the catalytic activity of the enzyme. These changes in the oxygen concentration can be indirectly used to determine other substrates. For example, glucose is widely determined by measuring changes in oxygen concentration produced during the catalytic activity of glucose oxidase [23, 24]. Other oxidases such as cholesterol oxidase, lactate oxidase, tyramine oxidase or urate oxidase (uricase) have been also widely used in this field [22, 25].

To develop biosensor membranes using optical oxygen transduction, a multifunctional material is required because it is necessary: 1) to immobilize a biomolecule which catalyses the oxidation of the analyte and 2) to incorporate an oxygen sensitive dye to measure the consumption of oxygen during this oxidation. Most biomolecules are hydrophilic compounds and require to be immobilised on hydrophilic supports in order to enhance its enzymatic activity [26]. On the other hand, oxygen sensitive dyes are hydrophobic compounds thus they have to be incorporated into hydrophobic supports to avoid aggregation and luminescence quenching by water which result in a decrease in sensitivity. Thus, the incorporation of both compounds in the same matrix maintaining their best analytical figures of merits is not trivial at all. Anyway, co-electrospinning technique allows the production of membranes with two different chemical environments; one hydrophobic to incorporate the oxygen sensitive dye and other hydrophilic to immobilize the biomolecule. In addition, this technique provides well-organised materials. It is important because the biomolecule must be located on the surface of the membrane to be accessible to the analyte while the oxygen sensitive dye must be incorporated into the membrane to avoid contact with water. Lastly, co-electrospinning also allows the production of this complex material in only one step, simplifying its scaling-up and therefore, its ability to be marketed.

In this work, we have developed and characterised a multifunctional coaxial material prepared from two different polymeric solutions by using co-electrospinning, which originates nonwoven nanofibre membranes with very large surface area, excellent mechanical properties (resistance to abrasion, high tensile strength, flexibility, easy handling) and high chemical resistance. It is based on an inner fibre containing an oxygen sensitive dye (Pd^{2+}-based porphyrin) and an outer fibre containing an appropriate chemical functionalization for immobilizing oxidase enzymes. After the immobilization of the enzyme, the sensing material preserves the oxygen sensing properties of the embedded dye and the immobilised enzyme is active.

In order to demonstrate its applicability, uricase has been selected as model enzyme and it has been used for determining uric acid in serum samples, obtaining similar results than those obtained with a reference method developed by an external laboratory. The good correlation obtained between both methods makes these nanofibre membranes a potential material for sensing applications.

2. Experimental

2.1. Chemicals

For the fabrication of the coaxial nanofibre membranes, PolymBlend®, (NanoMyP®, Granada, Spain, http://www.nanomyp.com), was used in the outer fibre and poly(methyl methacrylate) (PMMA) (Sigma Aldrich, Madrid, Spain) was used for the inner fibre. In addition, several oxygen sensitive dyes were also tested: Pt(II) meso-tetra(pentafluorophenyl)porphine (PtTFPP) (Frontier Scientific, Logan, UT, USA), Pd(II) meso-tetra(pentafluorophenyl)porphine (PdTFPP) (Frontier Scientific, Logan, UT, USA), Pt(II)-5-(4-bromophenyl)-10,15,20-tri(phenyl)-tetrabenzoporhyrin (PtTPTBPBr) which was synthesised following the procedure described by [27], and $[Ir(npy)_2(bpy\text{-}pyr_2)]PF_6$ (npyH= 2-(naphthalen-1-yl)pyridine; bpy= 2,2'-bipyridine; pyr= pyrene) (IrBPY) which was synthesised following the procedure described by [28]. Finally, N,N-dimethylformamide (DMF) (Sigma Aldrich, Madrid, Spain) was used as solvent for the outer and inner polymeric mixtures.

For the immobilization of uricase, ethylenediamine (EDA), glutaraldehyde (GA), potassium dihydrogen phosphate (KH_2PO_4), boric acid (H_3BO_3), glycine, uricase from *Candida* sp. (EC 1.7.3.3) and Tween 20 were all purchased from Sigma Aldrich, Madrid, Spain and used without further purification. All the solutions were prepared using doubly distilled water.

To assay the activity of uricase, 4-aminoantipyrine (4-AAP) and peroxidase (HRP) from horseradish (EC 1.11.1.7) were purchased from Sigma Aldrich, Madrid, Spain, and uric acid and sodium 3,5-dichloro-2-hydroxybenzenesulfonate (DCHBS) were purchased from Alfa Aesar, Karlsruhe, Germany.

Human serum samples were obtained from a clinical analysis laboratory and stored frozen until assay.

2.2. Instrumentation

The UV-Visible absorption spectra were recorded on a Varian Cary 50 UV-Vis spectrophotometer. The luminescence measurements were carried out on a Varian Cary-Eclipse luminescence spectrophotometer.

To characterize the optical properties of the materials, a flow cell which allows the use of a gas stream was used in order to perform the measurements in a controlled atmosphere. The gas stream was controlled with a mass-flow controller (MFC) (EL-FLOW Select F-201CV, Bronkhorst High-

Tech, Ruurlo, Netherlands) connected with the flow cell using copper and stainless steel tubing and a PC via a RS-232 serial port by a Flow-Bus Interface (Bronkhorst High-Tech Ruurlo, Netherlands).

All the luminescence measurements were carried out by controlling the temperature, which was continuously regulated by a commercial Peltier cell holder connected to a temperature control module (Agilent Technologies, Madrid, Spain).

The pH of the buffer solutions was controlled using a digital pH meter (Crison micropH 2000) calibrated at 20 ± 2 ºC.

2.3. Fabrication of multifunctional coaxial fibre membranes

To make coaxial fibres by co-electrospinning different solutions for inner and outer fibres were used. The liquid flow rates formed by outer and inner solutions were independently driven by two syringe pumps (Cole Parmer 74900 Series) using a flow-rate of 1.3 and 0.3 mL h^{-1} for the outer and inner solutions, respectively. The syringes used are Teflon Becton & Dickinson with 12.45 mm diameter. The outer and inner solutions were passed through a Teflon capillary tube until reaching a concentric couple of stainless-steel capillary tubes (injector). The outer and inner diameters of stainless-steel capillary tubes were: external tube Φ_{ext}/Φ_{int}=1.7/1.4 mm, internal tube Φ_{ext}/Φ_{int}=1/0.7 mm. To apply the electric field, two high-voltage power supplies were used (Gamma High Voltage ES30P and Bertan 205B-10R) to establish a potential difference between the injector and the collector which was a rotator drum (30 cm length and 20 cm diameter rotating at 400 rpm) located 25 cm apart from the injector. One of the power supplies was connected to the injector in positive polarity (8.9 kV) with respect to ground while the second power supply was hooked to the collector and run in negative polarity (-1.3 kV) with respect to ground. The selected flow rates and voltages within this configuration allowed the collection of dry fibre mats. The process was run for 8 h to collect membranes with thickness about 150 µm.

The obtained membrane is hydrophobic but when it is introduced in warm water at 40ºC (thermal wetting) the hydration is produced and the material is transformed in a very high hydrophilic membrane; during the thermal wetting the membrane must be keep stretched in order to prevent shrinks. It happens because during the thermal wetting the polymeric chains suffer a rearrangement and the hydrophilic domains of the polymeric chains are exposed to water while the hydrophobic domains are hidden to water [29]. Therefore at the end of the thermal wetting the surface of the mat reaches a high concentration of hydroxyl groups transforming the membrane in a very hydrophilic material without producing any change in diameter and fibre morphology [30]. After thermal wetting

the water absorption capacity was determined by calculating the ω parameter (amount of absorbed water per mass of material) [29]. It was 2.0 for the membrane with thermal wetting and 0.0 for the membrane without the thermal wetting.

The resulting coaxial-nanofibre membranes after the thermal wetting were attached to adhesive sheets (Lohmann Technologies Corp.) to facilitate their handling.

2.4. Characterization of multifunctional coaxial fibre mats

The morphological characterization of coaxial fibre membranes was done by TEM (Zeiss DSM 950) and SEM (LEO, Carl Zeiss, GEMINI-1530).

The oxygen sensing properties of the coaxial membranes were evaluated by applying different O_2 partial pressures, which were obtained by mixing O_2 and N_2 with different flow ratios, assuming a constant environmental pressure of 1000 mbar. The standard settings for the luminescence intensity measurements were: excitation and emission slits of 10 nm wide, delay time (t_d) 200 µs, gate time (t_g) 5 ms, and a current flow of 150 mL min^{-1}. Different emission and excitation wavelengths were selected for each oxygen-sensitive dye (see Table 1).

Table 1

Maxima luminescence excitation and emission wavelengths ($\lambda_{exc/em}$) and oxygen sensitivity of the dyes (K_{SV}) incorporated into the coaxial nanofibre membrane and in a classical PS membrane.

	Coaxial nanofibre membrane (this work)		**Classical PS membrane**		
Oxygen dye	**$\lambda_{exc/em}$ (nm)**	**K_{SV} (bar^{-1})**	**$\lambda_{exc/em}$ (nm)**	**K_{SV} (bar^{-1})**	**Reference**
PtTFPP	390/648	5.41	395/650	41.42	[31]
PdTFPP	402/669	20.84	406/671	9.60	[32]
PtTPTBPBr	614/767	5.26	614/770	22.8	[27]
IrBPY	334/577	13.60	334/557	8.79	[28]

Luminescence quenching methods of analysis can be described by the Stern–Volmer equation (see Eq. 1) which was used to fit the calibration curves for the oxygen sensing membranes.

$$\frac{I_0}{I} = 1 + K_{SV} pO_2 \qquad (1)$$

where I_0 and I are the luminescence emission intensities from the membranes exposed to 100% N_2 concentration and to different O_2 concentrations, respectively, K_{SV} is the Stern-Volmer constant and pO_2 is the oxygen partial pressure.

2.5. Immobilization of uricase

The surface of the coaxial material was first functionalised with a vinyl active group [33] and then with amino groups by using 0.9 M EDA in phosphate buffer (100 mM, pH 8.4) for 20 min at room temperature (RT) [34]. After this, 1.9 cm^2 of material were incubated with 5 mL of GA [34] solution 3 % v/v in phosphate buffer (100 mM, pH 7.4) for 40 min at RT in a rotating shaker. Then, it was washed with 5 mL of doubly distilled water (3x10 min in a rotating shaker).

The covalent immobilization of uricase on the material was carried out by incubating 1.9 cm^2 of activated material with 4 mL uricase solution (25 µg mL^{-1}) in phosphate buffer (50 mM, pH 7.4) at 4 ºC for 20 h. Unbound enzyme was removed by washing the material with 4 mL phosphate buffer (3x10 min in a rotating shaker). The washing solutions and the reaction supernatant were reserved for further testing. The material with immobilised uricase was stored in phosphate buffer (pH 7.4) at 4 ºC.

The amount of enzyme immobilised on the material was calculated from the difference between the initial free enzyme amount and the total amount of enzyme present in the reaction supernatant and washing solutions after immobilization, assuming that the loss of enzyme in each experiment is negligible. The enzyme concentrations in the supernatant and washing solutions were measured by the spectrofluorometric method at 334 nm [35].

The relative activity (%) of the immobilised uricase was determined by a colorimetric method based on two enzymatic reactions [36]. First, uricase catalyses the oxidation of uric acid to allantoin, carbon dioxide and hydrogen peroxide. Next, HRP catalyses the oxidation of DCHBS in the presence of hydrogen peroxide, which originates a phenoxyl radical that reacts with 4-AAP, producing a red quinoneimine dye with an absorption maximum at 515 nm. The relative activity of uricase was calculated as a percentage of the immobilised uricase referred to free uricase activities.

In detail, to assay the activity of the immobilised uricase, 3 mL glycine buffer (50 mM, pH 8.8) containing 0.1 µmol uric acid were incubated with 1.9 cm^2 of coaxial membrane with immobilised uricase for 20 min at 40 ºC. Next, 0.5 mL 4-AAP (10 mM), 0.5 mL DCHBS (50 mM) and 0.5 mL HRP (20 U mL^{-1}) in phosphate buffer (50 mM, pH 7.4) were added and kept at 40 ºC for 5 min to develop the colour. All the solutions were freshly prepared daily.

2.6. Analytical characterization and application

The luminescence signal of the oxygen sensitive dye incorporated into the inner fibre increases with the concentration of uric acid due to the consumption of oxygen during the oxidation reaction. SM shows the typical format of the evolution of the luminescence versus time (see SM, Fig. SM-1). As shown in SM, Fig. SM-1a, it provides a plateau in a very long period of time. In order to avoid large analysis times, the slope of this signal was used as sensing response (see SM, Fig. SM-1b).

The slope of the signal can be calculated with the following equation (see Eq. 2):

$$Sensing\ response = \frac{S_i - S_0}{t_i - t_0} \quad (2)$$

where S_i and S_0 are the luminescence signal recorded at time t_i and t_0, respectively, and t_0 must be equal o higher than the time in which the uric acid is added.

The calibration curve and the sample measurements were done by immersing the coaxial membranes in 600 µL of glycine buffer (50 mM, pH=8.8) and then 100 µL of uric acid solutions at different concentrations or serum sample were added, maintaining the temperature at 40 ºC during the measurement. The luminescence intensity was measured at $\lambda_{exc/em}$ = 402/669 nm, t_d = 200 µs, t_g = 5 ms, detector voltage 680 V and excitation and emission slits of 10 nm wide.

In order to demonstrate the capacity of the developed sensing membrane for determining uric acid, 4 real serum samples were analysed. The concentration of uric acid in the serum samples was also determined by an external laboratory (Análisis Clínicos Gilabert, Granada, Spain) by using the following colorimetric enzymatic method: uric acid is oxidised by uricase to allantoine and hydrogen peroxide ($2H_2O_2$), which under the influence of peroxidase (HRP), 4-aminophenazone (4-AP) and 2-4-dichlorophenol sulfonate (DCPS) forms a red quinoneimine compound (λ_{max}=520 nm):

$$Uric\ acid + 2H_2O + O_2 \xrightarrow{Uricase} Allantoine + 2H_2O_2$$

$$DCPS + 2H_2O_2 + 4\text{-}AP \xrightarrow{POD} Quinoneimine + 4H_2O$$

The intensity of the red colour formed is proportional to the uric acid concentration in the sample.

3. Results and discussion

3.1. Fabrication of the multifunctional coaxial membrane

The development of biosensor membranes using optical oxygen transduction requires a material with 2 functionalities: 1) it must allow the immobilization of a biomolecule on its surface to catalyse the oxidation of the analyte; and 2) it must contain an oxygen sensitive dye to measure the consumption of oxygen during this oxidation. In addition, due to the different character of the biomolecule (hydrophilic) and the oxygen sensitive dye (hydrophobic), this bi-functional material has to contain two different chemical environments: a hydrophilic environment for the enzyme and a hydrophobic environment for the oxygen-sensitive dye.

In order to obtain the hydrophilic environment, PolymBlend® was selected for the outer polymer solution because it is hydrophilic and oxygen permeable, it contains OH groups that can be easily functionalised to allow the covalent immobilization of the enzyme, and it has been formulated with an optimum mixture of two high molecular weight statistic copolymers to provides excellent mechanical and chemical properties of non-woven mats produced by electrospinning [37, 38]. The use of this polymer blend provides to the coaxial materials similar properties than those observed in single fibre, nonwoven mats produced with these polymer; among others, resistance to acid and bases in a wide pH range (3.5 -12.0), temperature resistance up to 100ºC and high resistance to water, hydrophobic solvents (such as toluene, vegetal oils, hexane) and to hydroalcoholic mixtures (up to 30 % v/v).

For the hydrophobic environment to incorporate the oxygen-sensitive dye, PMMA was selected because it is hydrophobic, compatible with the oxygen sensitive dyes, oxygen permeable, it has a good transparency to allow the luminescence measurement and it was proved to be good polymer for developing oxygen sensing membranes by electrospinning [20].

Concerning the oxygen sensitive dye, there is a huge variety of optical indicators with different structures and chemical nature to determine oxygen [39] and most of them are based on the measurement of the luminescence quenching produced by oxygen [40].

Organometallic complexes containing Ru^{2+}, Re^{+}, Os^{3+}, Ir^{3+}, Pt^{2+} and Pd^{2+} as well as with polypyridyl and porphyrin structures are the most widely used compounds as oxygen-sensitive dyes in optical sensing. There are a vast number of these complexes with different physicochemical properties, emission and excitation wavelengths, lifetimes, Stokes' shifts, quantum yields, photostability, etc. [39, 40]. Thus, the selection of the most adequate oxygen dye would mainly

depend on the application of the sensor, taking into account factors like oxygen sensitivity and stability.

In this work, we have selected two commercially available metalloporphyrins (PtTFPP and PdTFPP), one modified Pt(II)–benzoporphyrin (PtTPTBPBr), and one cyclometalated Ir(III) complex ($[Ir(npy)_2(bpy\text{-}pyr_2)]PF_6$), as oxygen-sensitive dyes. These three dyes show exceptional luminescence properties and they are completely compatible with the polymeric solution (PMMA in DMF) used to obtain the inner fibre of the coaxial membranes.

To produce a stable and continuous co-electrospinning procedure, we tested two different concentrations (13 and 10% w/w) of PolymBlend® in the outer fluid and three concentrations (13, 9 and 6% w/w) of PMMA in the inner fluid. We selected 10% w/w of PolymBlend® and 6% w/w of PMMA as optimum concentrations because they provide a stable and definite cone and they help to solidify the electrified jet near its point of generation (see SM, Fig. SM-2). The percentage of the polymer in the outer solution is higher because a sufficiently high viscosity of the outer fluid is essential to develop a compound cone in the steady state. In addition, it helps to increase the polymeric chain entanglements which prevent various instabilities (break up of the jet into droplets).

In this work, to develop a compound cone in the steady state, we studied different outer/inner flow rates (1/0.2, 1.3/0.1, 1.3/0.3, 1.3/0.5, and 2.5/0.5 mL h^{-1}, respectively), optimizing the injector/collector voltages for each of them; the optimum injector/collector voltages were10.3/-0.6, 9.5/-1.7, 8.9/-1.3, 8.8/-2.6, and 10.0/-1.7 kV, respectively. The optimal voltages were selected by using a high resolution camera and selecting the voltages for each outer/inner flow rate which provide a stable cone. The optimal conditions for obtaining the coaxial nanofibre mat were: outer and inner flow rates of 1.3 and 0.3 mL h^{-1}, which need an injector voltage of 8.9 kV and collector voltage of -1.3 kV (see SM, Fig. SM-3).

Fig. 1 and SM (see Fig. SM-2) show SEM and TEM pictures of the optimal coaxial nanofibre mat. They show a regular and homogeneous formation of the fibres during the co-electrospinning procedure. The addition of 1% w/w of the O_2 indicator into the inner suspension did not affect the co-electrospinning process, and thus the morphology of the coaxial fibres did not change. No leaching of the dyes from the membrane was observed and all the coaxial mats showed similar mechanical properties. SM (see Fig. SM-4) shows the luminescence emission before and after the thermal wetting of the mat. The luminescence emission is the same before and after the treatment therefore we can assume that the dye was not leached during this procedure.

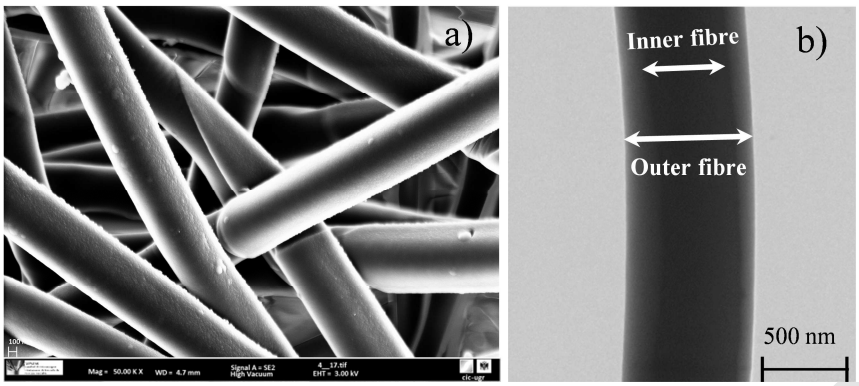

Fig. 1. Images of a) SEM and b) TEM of the multifunctional coaxial membrane formed by PMMA-PdTFPP as inner fibre and PolymBlend® as outer fibre.

The fibre diameters of the obtained coaxial fibres are 680 and 530 nm for outer and inner fibres, respectively. These values were calculated by 20 measurements made in five different SEM pictures (total of 100 measurements).

3.2. Optical characterization and oxygen sensing properties

A coaxial membrane was produced containing several dyes in order to evaluate the effect of the incorporation of a dye into the inner fibre of the material. The emission and excitation spectra of the coaxial materials based on the different oxygen dyes (1 % w/w) and under different oxygen concentrations are shown in Fig. 2, Table 1 and SM (see Fig. SM-5). The luminescence properties of the dyes incorporated into the inner fibre of the coaxial material are very similar to those obtained in a classical PS membrane (see Table 1), thus the incorporation of the dye into a nanofibre mat produced by co-electrospinning does not affect its optical properties.

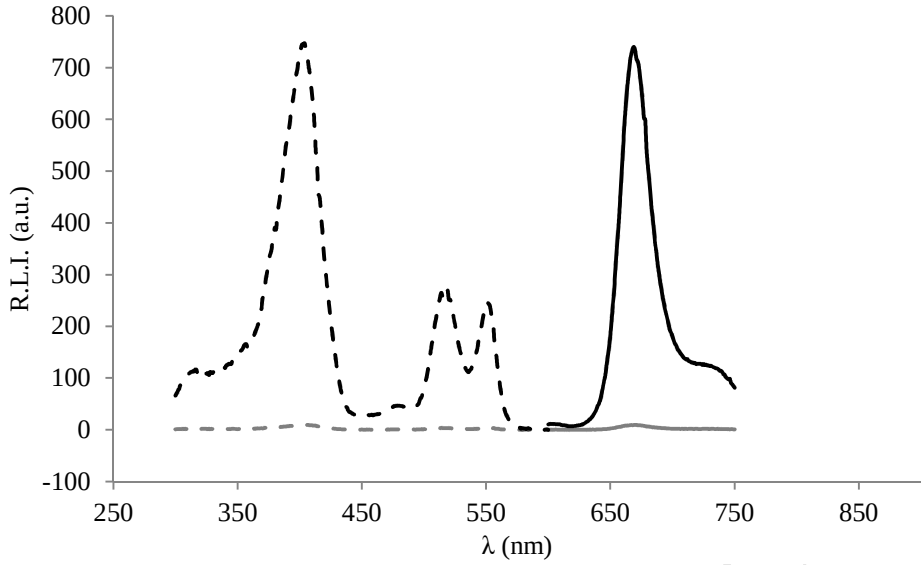

Fig. 2. Excitation (dashed line) and emission (solid line) spectra in the presence of 100% O_2 (grey line) and 100% N_2 (black line) of the coaxial membrane when PdTFPP was used as oxygen sensitive dyes. [Dye concentration] = 1% w/w, t_d=200µs, t_g=5 ms and monochromator slitwidth$_{exc/em}$=10/10 nm.

Concerning the sensitivity to oxygen, all the obtained Stern-Volmer plots (see SM, Fig. SM-6) showed linearity up to 10% of oxygen concentration so all of them might be used as optical oxygen sensing. Table 1 also shows the sensitivity (K_{SV}) of the coaxial membranes. Comparing the sensitivity to oxygen of the different dyes incorporated into the coaxial membranes and in a classical membrane (PS membrane), it is possible to conclude that the K_{SV} of the coaxial fibre mats based on Pt(II) complexes are smaller than those of the classical membranes meanwhile the K_{SV} of the coaxial fibre mats based on Pd(II) and Ir(III) complexes are higher than those of the classical membranes (see Table 1). It can be due to aggregation of Pt(II) dyes during the electrospinning process while PdTFPP and IrBPY are more soluble in PMMA than in PS. Anyway, the obtained sensitivity is enough for the requested application and it might be improved, if necessary, by using advanced photoluminescence measurements such as the use of rectangular-wave signals [41].

Analysing the results summarised in Table 1, PdTFPP showed the highest sensitivity to oxygen thus it was selected as the oxygen-sensitive dye on the fabrication of the multifunctional material.

3.3. Optimization of covalent immobilization of the enzyme on coaxial membrane

The immobilization of enzymes whose catalytic activity involves the consumption or the production of oxygen, such as oxidases, on oxygen-sensitive membranes can be used to develop biosensors that determine the substrates of the enzymatic reactions. To demonstrate the versatility of the proposed material, uricase was selected as model enzyme and the resulting membrane was used to analyse uric acid by oxygen transduction.

Uricase was covalently immobilised on the outer surface of the coaxial material through the formation of Schiff bases between the amino groups of the enzyme and the free aldehyde groups of GA on the material. Therefore, the OH groups of the outer polymer fibres was first functionalised with vinyl active groups, then with amino groups by using EDA and finally with GA [34].

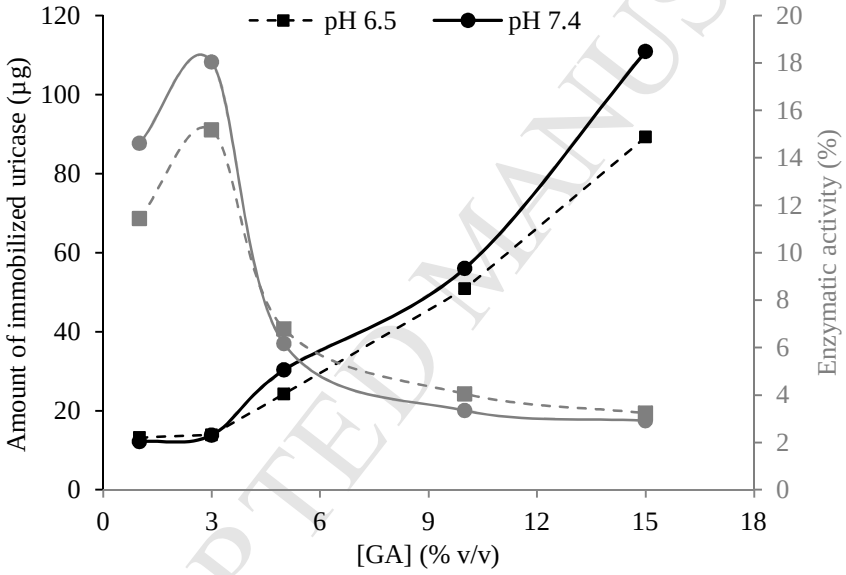

Fig. 3. Effect of the concentration of GA on the amount (black line) and enzymatic activity (grey line) of immobilised uricase at pH 7.4 (experimental data indicated with a solid circle) and pH 6.5 (experimental data indicated with a solid square).

The optimum GA concentration was assayed by incubating the material with solutions containing 1, 3, 5, 10 and 15 % v/v GA in phosphate buffer (100 mM, pH 6.5 and 7.4) for 40 min at RT, and then immobilizing uricase in phosphate buffer (50 mM, pH 7.4) at 4 ºC for 20 h. Fig. 3 shows that an increase of the GA concentration from 3 to 15 % v/v provides an increase of the immobilised enzyme but also a considerable decrease of the activity. It is because an increase of the GA concentration provides an increase of the amount of aldehyde groups that can react with the enzyme and therefore an increase of the amount of enzyme which has been covalently immobilised on the

material. But, at the same time, an increase of the amount of aldehyde groups also provides that the multipoint attachment of the enzyme occurs more extensively and, therefore, the rigidity of the enzyme is increased, changing its conformation and therefore reducing its activity [42].

The reaction time with GA was also tested. SM (see Fig. SM-7) shows that the incubation time has a similar effect over the enzyme immobilization than the GA concentration; an increase in the reaction time from 40 min to 2 h provides an increase in the immobilised enzyme but the activity is decreased. Thus, the best relationship between activity and amount of immobilised enzyme was obtained at 3 % v/v GA and 40 min reaction time, which were selected as optimum GA concentration and incubation time, respectively. These conditions provide an immobilization yield of 7.4 μg cm^{-2} and an enzymatic activity of 18 % of the native enzymatic activity (activity of the free enzyme).

The effects of reaction time and temperature on the enzyme immobilization were also studied. The GA activated material was immersed in 4 mL uricase solution (25 μg mL^{-1}) in phosphate buffer (50 mM, pH 7.4) at 4 and 25 ºC for different reaction times. Then the amount of immobilised enzyme and its activity were evaluated. SM (see Fig. SM-8) shows the experimental results. The maximum amount of immobilised enzyme was reached at 25 ºC, but at this temperature the activity of the immobilised enzyme practically disappears. Thus, 4ºC was selected as optimum temperature for enzyme incubation. On the other hand, an increase of the incubation time at 4ºC provides an increase of the amount of the immobilised enzyme but a decrease in its activity. However, 20 h was selected in order to have a good amount of immobilised enzyme to increase the accuracy of the analytical determination.

To determine the influence of the pH, the immobilization of uricase on the activated material was carried out at pH=6.5 (50 mM phosphate buffer), pH=7.4 (50 mM phosphate buffer), pH=8.8 (50 mM borate buffer) and pH=8.8 (50 mM glycine buffer) at 4 ºC for 20 h. As can be seen in SM (see Fig. SM-9), the pH significantly affects both the amount and activity of the immobilised enzyme. The amount of immobilised enzyme increases with the pH, but the activity decreases considerably. It can be due to the change of the spatial conformation of the enzyme with the pH. The highest activity of the free enzyme is reached at pH 8.5 [43], and at this pH the active sites of the enzyme are more accessible so it is easier that at this pH the active site can interact with the aldehyde groups of GA and can be modified. Therefore, pHs close to 8.5 are not adequate to carry out the covalent immobilization on the material.

When the pH is between 6.5 and 7.4 the amount and the activity of the immobilised enzyme is practically the same, so phosphate buffer at pH 7.4 was selected as the optimum medium for developing the immobilization of uricase.

Finally, the effect of the enzyme concentration was also investigated. 4 mL uricase solutions with four different concentrations (25, 50, 100 and 150 µg mL^{-1}) in phosphate buffer (50 mM, pH 7.4) were incubated with the GA activated material at 4 ºC for 20 h. SM (see Fig. SM-10) shows the experimental results. An increase of the initial enzyme concentration increases the amount of the immobilised enzyme and decreases the activity. It could be due to the formation of aggregates when the enzyme concentration increases; an increase of the enzyme concentration increases the probability of the aggregation of the enzyme on the surface of the material, which might originate the blockage of their active sites. Thus, 25 µg mL^{-1} were selected as optimum uricase concentration providing an immobilization yield of 7.4 µg cm^{-2} and an enzymatic activity of the 18 % of the native enzymatic activity (activity of the free enzyme).

3.4. Analytical figures of merits

For the analytical characterization of uric acid, the coaxial membrane was immersed in glycine buffer (50 mM, pH=8.8) because, as it was commented before, this is the best medium to obtain the maximum activity of the enzyme [43] and then different concentrations of uric acid were added. The luminescence responses obtained for different uric acid concentrations in buffer solutions increase with the time and provide a plateau at a very long period of time (see Fig. SM-1). In order to avoid large analysis times, the slope of this signal was used as sensing response following the procedure described in section 2.6.

Table 2

Analytical figures of merits of the coaxial nanofibre membrane based on an inner fibre composed by PdTFPP/PMMA and an outer fibre composed by PolymBlend® functionalised with uricase in the optimal conditions.

	Estimated value
Linearity (%)	99.25
Slope (µM^{-1})	0.1133
Intercept	19.404
Linear range (µM)	15-500
Limit of detection (µM)	4
Limit of quantification (µM)	15

A linear relationship between the sensing response and the uric acid concentration was obtained in the range from 15 to 500 µM (see SM, Fig. SM-11), which covers the normal range in human serum (150-460 µM). Table 2 summarizes the analytical figures of merits of the proposed biosensing membrane. The detection and quantification limits were calculated by using the IUPAC method (LOD=3s_b/m; LOQ=10s_b/m).

In spite of the low relative activity of the immobilised uricase (18 %) and the small K_{SV} (20.84 bar^{-1}) of the dye incorporated into the coaxial membrane, they are enough to determine uric acid in real serum samples. In comparison with other biosensors previously published, see Table 3, the proposed one has a LOD in the same order of magnitude but the linear range is shorter; however it is good enough for uric acid determination in human serum. Anyway, further optimisation of the sensing material can be done in order to increase the sensitivity on those applications that need it. For example, the amount of dye can be reduced in order to avoid agglomeration and it might increase significantly the sensitivity to oxygen.

Table 3

Comparison of the proposed biosensor with other previously published in the literature.

Detection method	**LOD (µM)**	**Linear range (µM)**	**Immobilization Method**	**Matrix**	**Ref.**
Amperometry	5	5-800	Crosslinking/adsorption	Chitosan, carbon nanotube and polyaniline	[44]
Amperometry	2	4.0-640	Covalent	Eggshell membrane	[45]
Amperometry	140	50-1000	Adsorption	Copper oxide	[46]
Amperometry	10	10-600	Covalent	Polyaniline	[47]
Amperometry	0.33	2-10	Entrapment	Mesoporous silica	[48]
Fluorometry	5	5-800	Entrapment	Polyurethane hydrogel	[22]
Fluorometry	25	10-1700	Sol-gel entrapment	Polyvinylalcohol	[49]
Spectrophotometry	50	50-500	Covalent	Polyethylene terephthalate	[50]
Spectrophotometry	5.67	5.67-110	Adsorption	Polyacrylonitrile modified with polyaniline	[51]
Chemiluminescence	5	10-1000	Affinity	Chitosan	[52]
Luminescence	4	15-500	Covalent	PolymBlend® and PMMA	This work

The re-usability of the material was evaluated by using the same membrane to determine the uric acid of several samples at the same concentration (100 µM). SM, see Fig. SM-12, shows the results. It can be concluded that the same membrane can be used 8 times without disturbing the uric acid determination.

3.5. Application

In order to determine the applicability of the designed multifunctional material in complex matrices, the uric acid concentration was measured in 4 serum samples from healthy adults using 3 different coaxial membranes per sample following the procedure described in section 2.6. To test the accuracy of the results, the values of uric acid concentration in the serum samples obtained with the developed biosensor were compared with those obtained by using a reference method (external laboratory). Table 4 summarizes the results. A good correlation coefficient (0.996) and the regression equation ($y = 1.063x - 14.164$) were calculated by comparing the concentrations of uric acid obtained by both methods (see SM, Fig. SM-13). Because no interfering species were found in the analysis of real human serums, it is possible to conclude that the immobilisation of the uricase on the developed multifunctional material does not affect the selectivity of the enzyme.

Table 4

Results of the acid uric determination by the proposed biosensor and an external reference laboratory.

Sample	**[uric acid] (µM) External reference laboratory**	**[uric acid] (µM) proposed biosensor[a]**
1	220.1	219.8 ± 13.8
2	190.4	192.5 ± 13.4
3	148.7	142.1 ± 14.2
4	220.1	217.3 ± 17.6

[a] 3 different membranes per sample were used to determine the uric acid concentration

4. Conclusions

In this study, we have successfully designed a multifunctional material with sensing properties. It is constituted by nanofibres with a coaxial morphology, which originates two different chemical environments: an inner hydrophobic environment and an outer hydrophilic environment. The high capacity of the outer fibre for immobilizing biomolecules combined with the ability of the inner fibre to entrap optical indicators, result in a material with a high versatility and applicability in many fields. In addition, the use of the coelectrospinning technique allows the production of this complex material in only one step, simplifying its scaling-up and therefore, its ability to the market.

In order to demonstrate the usefulness of this material, uricase and PdTFPP were selected as biomolecule and optical indicator, respectively. Several chemical parameters have been optimised in order to achieve the best analytical figures. The obtained biosensing membrane provides a detection limit of 4 µM and a linear range of 15-500 µM, which allow determining uric acid in serum samples. The obtained results showed a good correlation (0.996) with those obtained by an external laboratory, which indicates that this material can be used as a promising sensing membrane. Moreover, it could also be used for the immobilization of other enzymes and for hosting other dyes, which could originate interesting applications in the field of biosensing.

Acknowledgments

This work has received funding from the People Programme (Marie Curie Actions, Multi-ITN) of the European Union's Seventh Framework Programme for research, technological development and demonstration under grant agreement n° 608104 (EUROMBR) and the Spanish Ministry of Economy and Competitiveness (Ramon-Marquez's grant reference AP2012-0944, Medina-Castillo's Torres Quevedo contract reference PTQ-11-04904 and project CTQ2014-53442-P). The authors also thank the research groups of E. Baranoff and I. Klimant for providing the IrBPY and PtTPTBPBr complexes, respectively, for this work.

Appendix A. Supplementary data

Supplementary data related to this article has been submitted.

References

[1] U. Agrawal, M. Gupta, R.S. Jadon, R. Sharma, S.P. Vyas, Multifunctional nanomedicines: potentials and prospects, Drug Delivery and Translational Research, 3 (2012) 479-497.
[2] G. Liu, Z. An, Frontiers in the design and synthesis of advanced nanogels for nanomedicine, Polymer Chemistry, 5 (2014) 1559-1565.

[3] H. Dai, Carbon Nanotubes: Synthesis, Integration, and Properties, Accounts of Chemical Research, 35 (2002) 1035-1044.
[4] Z. Ouyang, J. Li, J. Wang, Q. Li, T. Ni, X. Zhang, H. Wang, Q. Li, Z. Su, G. Wei, Fabrication, characterization and sensor application of electrospun polyurethane nanofibers filled with carbon nanotubes and silver nanoparticles, Journal of Materials Chemistry B, 1 (2013) 2415-2424.
[5] J.P. Rao, K.E. Geckeler, Polymer nanoparticles: Preparation techniques and size-control parameters, Progress in Polymer Science, 36 (2011) 887-913.
[6] H. Ghanbari, B.G. Cousins, A.M. Seifalian, A Nanocage for Nanomedicine: Polyhedral Oligomeric Silsesquioxane (POSS), Macromolecular Rapid Communications, 32 (2011) 1032-1046.
[7] N. Saifuddin, A.Z. Raziah, A.R. Junizah, Carbon Nanotubes: A Review on Structure and Their Interaction with Proteins, Journal of Chemistry, 2013 (2013) 18.
[8] R. Wu, K. Zhou, C.Y. Yue, J. Wei, Y. Pan, Recent progress in synthesis, properties and potential applications of SiC nanomaterials, Progress in Materials Science, 72 (2015) 1-60.
[9] B. Xu, R.G. Song, C. Wang, Preparation and characterization of Ag, Au and Ti metal nanoparticles colloids by pulsed laser ablation in liquids, Advanced Materials Research, 2012, pp. 648-651.
[10] X. Cui, S. Zhong, H. Wang, Emulsifier-free core-shell polyacrylate latex nanoparticles containing fluorine and silicon in shell, Polymer, 48 (2007) 7241-7248.
[11] S.T. Camli, F. Buyukserin, O. Balci, G.G. Budak, Size controlled synthesis of sub-100 nm monodisperse poly(methylmethacrylate) nanoparticles using surfactant-free emulsion polymerization, Journal of Colloid and Interface Science, 344 (2010) 528-532.
[12] S. Kruss, A.J. Hilmer, J. Zhang, N.F. Reuel, B. Mu, M.S. Strano, Carbon nanotubes as optical biomedical sensors, Advanced Drug Delivery Reviews, 65 (2013) 1933-1950.
[13] A. Oliveros, A. Guiseppi-Elie, S.E. Saddow, Silicon carbide: a versatile material for biosensor applications, Biomedical Microdevices, 15 (2013) 353-368.
[14] F.E. Ahmed, B.S. Lalia, R. Hashaikeh, A review on electrospinning for membrane fabrication: Challenges and applications, Desalination, 356 (2015) 15-30.
[15] N. Bhardwaj, S.C. Kundu, Electrospinning: A fascinating fiber fabrication technique, Biotechnology Advances, 28 (2010) 325-347.
[16] A. Baranowska-Korczyc, K. Sobczak, P. Dluzewski, A. Reszka, B.J. Kowalski, L. Klopotowski, D. Elbaum, K. Fronc, Facile synthesis of core/shell ZnO/ZnS nanofibers by electrospinning and gas-phase sulfidation for biosensor applications, Physical Chemistry Chemical Physics, 17 (2015) 24029-24037.
[17] R. Xue, C. Ge, K. Richardson, A. Palmer, M. Viapiano, J.J. Lannutti, Microscale Sensing of Oxygen via Encapsulated Porphyrin Nanofibers: Effect of Indicator and Polymer "Core" Permeability, ACS Applied Materials & Interfaces, 7 (2015) 8606-8614.
[18] Y. Liu, Q. Ma, M. Yang, X. Dong, Y. Yang, J. Wang, W. Yu, G. Liu, Flexible hollow nanofibers: Novel one-pot electrospinning construction, structure and tunable luminescence–electricity–magnetism trifunctionality, Chemical Engineering Journal, 284 (2016) 831-840.
[19] F. Bi, X. Dong, J. Wang, G. Liu, Tunable and enhanced simultaneous magnetism-luminescence bifunctionality assembled into a coaxial nanofiber, New Journal of Chemistry, 39 (2015) 3444-3451.
[20] A.L. Medina-Castillo, J.F. Fernández-Sánchez, A. Fernández-Gutiérrez, One-Step Fabrication of Multifunctional Core-Shell Fibres by Co-Electrospinning, Advanced Functional Materials, 21 (2011) 3488-3495.
[21] Z. Sun, E. Zussman, A.L. Yarin, J.H. Wendorff, A. Greiner, Compound Core–Shell Polymer Nanofibers by Co-Electrospinning, Advanced Materials, 15 (2003) 1929-1932.
[22] P. Schrenkhammer, O.S. Wolfbeis, Fully reversible optical biosensors for uric acid using oxygen transduction, Biosensors and Bioelectronics, 24 (2008) 994-999.
[23] M.-S. Steiner, A. Duerkop, O.S. Wolfbeis, Optical methods for sensing glucose, Chemical Society Reviews, 40 (2011) 4805-4839.

[24] G. Chang, Y. Tatsu, T. Goto, H. Imaishi, K. Morigaki, Glucose concentration determination based on silica sol–gel encapsulated glucose oxidase optical biosensor arrays, Talanta, 83 (2010) 61-65.
[25] H.D. Duong, J.I. Rhee, Preparation and characterization of sensing membranes for the detection of glucose, lactate and tyramine in microtiter plates, Talanta, 72 (2007) 1275-1282.
[26] J.N. Talbert, J.M. Goddard, Enzymes on material surfaces, Colloids and Surfaces B: Biointerfaces, 93 (2012) 8-19.
[27] L.H. Hutter, B.J. Muller, K. Koren, S.M. Borisov, I. Klimant, Robust optical oxygen sensors based on polymer-bound NIR-emitting platinum(ii)-benzoporphyrins, Journal of Materials Chemistry C, 2 (2014) 7589-7598.
[28] S. Medina-Rodriguez, S.A. Denisov, Y. Cudre, L. Male, M. Marin-Suarez, A. Fernandez-Gutierrez, J.F. Fernandez-Sanchez, A. Tron, G. Jonusauskas, N.D. McClenaghan, E. Baranoff, High performance optical oxygen sensors based on iridium complexes exhibiting interchromophore energy shuttling, Analyst, 141 (2016) 3090-3097.
[29] A. Stathopoulos, P. Klonos, A. Kyritsis, P. Pissis, C. Christodoulides, J.C. Rodriguez Hernández, M. Monleón Pradas, J.L. Gómez Ribelles, Water sorption and polymer dynamics in hybrid poly(2-hydroxyethyl-co-ethyl acrylate)/silica hydrogels, European Polymer Journal, 46 (2010) 101-111.
[30] A.J. Campillo-Fernández, M. Salmerón Sánchez, R. Sabater i Serra, J.M. Meseguer Dueñas, M. Monleón Pradas, J.L. Gómez Ribelles, Water-induced (nano) organization in poly(ethyl acrylate-co-hydroxyethyl acrylate) networks, European Polymer Journal, 44 (2008) 1996-2004.
[31] S. Medina-Rodriguez, M. Marin-Suarez, J.F. Fernandez-Sanchez, A.d.l. Torre-Vega, E. Baranoff, A. Fernandez-Gutierrez, High performance optical sensing nanocomposites for low and ultra-low oxygen concentrations using phase-shift measurements, Analyst, 138 (2013) 4607-4617.
[32] S.M. Borisov, I. Klimant, Luminescent nanobeads for optical sensing and imaging of dissolved oxygen, Microchimica Acta, 164 (2008) 7.
[33] A.L. Medina-Castillo, J. Morales-Sanfrutos, A. Megia-Fernandez, J.F. Fernandez-Sanchez, F. Santoyo-Gonzalez, A. Fernandez-Gutierrez, Novel synthetic route for covalent coupling of biomolecules on super-paramagnetic hybrid nanoparticles, Journal of Polymer Science Part A: Polymer Chemistry, 50 (2012) 3944-3953.
[34] J.M. Goddard, J.H. Hotchkiss, Polymer surface modification for the attachment of bioactive compounds, Progress in Polymer Science, 32 (2007) 698-725.
[35] M.S. Caves, B.K. Derham, J. Jezek, R.B. Freedman, Thermal Inactivation of Uricase (Urate Oxidase): Mechanism and Effects of Additives, Biochemistry, 52 (2013) 497-507.
[36] T. Ramon-Marquez, A.L. Medina-Castillo, J.F. Fernandez-Sanchez, A. Fernandez-Gutierrez, Evaluation of different functional groups for covalent immobilization of enzymes in the development of biosensors with oxygen optical transduction, Analytical Methods, 7 (2015) 2943-2949.
[37] T. Ramon-Marquez, A.L. Medina-Castillo, A. Fernandez-Gutierrez, J.F. Fernandez-Sanchez, A novel optical biosensor for direct and selective determination of serotonin in serum by Solid Surface-Room Temperature Phosphorescence, Biosensors and Bioelectronics, 82 (2016) 217-223.
[38] T. Ramon-Marquez, A.L. Medina-Castillo, A. Fernandez-Gutierrez, J.F. Fernandez-Sanchez, Novel optical sensing film based on a functional nonwoven nanofibre mat for an easy, fast and highly selective and sensitive detection of tryptamine in beer, Biosensors and Bioelectronics, 79 (2016) 600-607.
[39] M. Quaranta, S.M. Borisov, I. Klimant, Indicators for optical oxygen sensors, Bioanalytical Reviews, 4 (2012) 115-157.
[40] X.-d. Wang, O.S. Wolfbeis, Optical methods for sensing and imaging oxygen: materials, spectroscopies and applications, Chemical Society Reviews, 43 (2014) 3666-3761.
[41] S. Medina-Rodríguez, Á. de la Torre-Vega, F.J. Sainz-Gonzalo, M. Marín-Suárez, C. Elosúa, F.J. Arregui, I.R. Matias, J.F. Fernández-Sánchez, A. Fernández-Gutiérrez, Improved

Multifrequency Phase-Modulation Method That Uses Rectangular-Wave Signals to Increase Accuracy in Luminescence Spectroscopy, Analytical Chemistry, 86 (2014) 5245-5256.
[42] L. Cao, Covalent Enzyme Immobilization, Carrier-bound Immobilized Enzymes, Wiley-VCH Verlag GmbH & Co. KGaA2006, pp. 169-316.
[43] L. Jianguo, L. Gaoxiang, L. Hong, Z. Xiukai, Purification and properties of uricase fromCandida sp. and its application in uric acid analysis in serum, Applied biochemistry and biotechnology, 47 (1994) 57-63.
[44] R. Rawal, S. Chawla, N. Chauhan, T. Dahiya, C.S. Pundir, Construction of amperometric uric acid biosensor based on uricase immobilized on PBNPs/cMWCNT/PANI/Au composite, International Journal of Biological Macromolecules, 50 (2012) 112-118.
[45] Y. Zhang, G. Wen, Y. Zhou, S. Shuang, C. Dong, M.M.F. Choi, Development and analytical application of an uric acid biosensor using an uricase-immobilized eggshell membrane, Biosensors and Bioelectronics, 22 (2007) 1791-1797.
[46] K. Jindal, M. Tomar, V. Gupta, CuO thin film based uric acid biosensor with enhanced response characteristics, Biosensors and Bioelectronics, 38 (2012) 11-18.
[47] K. Arora, G. Sumana, V. Saxena, R.K. Gupta, S.K. Gupta, J.V. Yakhmi, M.K. Pandey, S. Chand, B.D. Malhotra, Improved performance of polyaniline-uricase biosensor, Analytica Chimica Acta, 594 (2007) 17-23.
[48] R. Mundaca-Uribe, F. Bustos-Ramírez, C. Zaror-Zaror, M. Aranda-Bustos, J. Neira-Hinojosa, C. Peña-Farfal, Development of a bienzymatic amperometric biosensor to determine uric acid in human serum, based on mesoporous silica (MCM-41) for enzyme immobilization, Sensors and Actuators B: Chemical, 195 (2014) 58-62.
[49] H.-c. Tsai, R.-a. Doong, Simultaneous determination of renal clinical analytes in serum using hydrolase- and oxidase-encapsulated optical array biosensors, Analytical Biochemistry, 334 (2004) 183-192.
[50] K. Phaugat, M. Bhambi, Renu, C.S. Pundir, Polyethylene terephthalate membrane as a support for covalent immobilization of uricase and its application in serum urate determination, Journal of Molecular Catalysis B: Enzymatic, 62 (2010) 27-31.
[51] G. Bayramoğlu, A.Ü. Metin, M.Y. Arıca, Surface modification of polyacrylonitrile film by anchoring conductive polyaniline and determination of uricase adsorption capacity and activity, Applied Surface Science, 256 (2010) 6710-6716.
[52] D. Yao, A.G. Vlessidis, N.P. Evmiridis, Microdialysis sampling and monitoring of uric acid in vivo by a chemiluminescence reaction and an enzyme on immobilized chitosan support membrane, Analytica Chimica Acta, 478 (2003) 23-30.

Highlights

- A coaxial multifunctional material for biosensors has been developed
- It allows the enzyme immobilisation and optical oxygen transduction
- It shows a detection limit of 4 µM and a linear range of 15-500 µM
- It has been used for detecting uric acid in serum samples